Description of magnetic interactions in strongly correlated solids via range-separated hybrid functionals

Pablo Rivero,[1] Ibério de P. R. Moreira,[1] Gustavo E. Scuseria,[2] and Francesc Illas[1]
[1]*Departament de Química Física and Institut de Química Teòrica i Computacional (IQTCUB), Universitat de Barcelona, C/Martí i Franquès 1, E-08028 Barcelona, Spain*
[2]*Department of Chemistry, Rice University, 6100 Main Street, Houston, Texas 77005-1892, USA*
(Received 20 February 2009; revised manuscript received 28 April 2009; published 25 June 2009)

The performance of two range-separated hybrid (HSE and LC-ωPBE) exchange-correlation functionals for describing narrow-band magnetic solids and, more precisely, for predicting magnetic coupling constants has been investigated for a large set of systems for which accurate experimental data exist. The set includes superconducting cuprates parent compounds and transition-metal oxides and fluorides exhibiting a broad range of magnetic coupling values. Both HSE and LC-ωPBE provide an overall improvement over the description arising from standard hybrid functionals such as the well-known B3LYP. Nevertheless, the two range-separated hybrid functionals still overestimate antiferromagnetic and ferromagnetic interactions although significantly less than B3LYP. The increased accuracy of LC-ωPBE suggests that the approximations and exact constraints included in the definition of this long-range corrected hybrid functional have important consequences for the accurate description of exchange and correlation effects of the electronic structure of magnetic solids and other systems exhibiting localized spins.

DOI: 10.1103/PhysRevB.79.245129 PACS number(s): 71.15.−m

I. INTRODUCTION

The discovery of high-temperature superconductivity in doped cuprates in 1986 (Ref. 1) sparked substantial interest in strongly correlated systems and triggered a huge amount of work from both theory and experiment.[2–6] In fact, superconducting cuprates provide one of the most typical examples of strongly correlated systems, a wide class of materials that show unusual electronic and magnetic properties. In solid-state physics, the term strong correlation is applied to emphasize the situations where the electrons tend to be localized and strongly interacting.[7] Consequently, the resulting electronic structure of these solids is not well-described, most often not even in a qualitatively correct manner, by simple one-electron theories such as the local-density approximation (LDA) of density-functional theory (DFT)[8–10] or even by the more sophisticated generalized gradient approaches,[11] usually referred to as GGA. This is somehow different from the meaning that electron correlation has in quantum chemistry where it is defined with respect to the Hartree-Fock model.[7,12] The apparently simple NiO is surely the archetype of strongly correlated materials, it has a partially filled $3d$ band with the Ni^{2+} cations almost in a $3d^8$ configuration and therefore from band theory arguments it would be expected to be a good conductor. However, taking into account the strong Coulomb repulsion between d electrons, an electron correlation effect, NiO appears to be predicted to behave as an antiferromagnetic wide band-gap insulator,[13] as observed in experiments. Thus, strongly correlated materials have electronic structures that do not follow simple free-electron-like models. A careful discussion about the limitations of current DFT methods was recently provided by Yang and co-workers.[14,15]

In spite of significant advances, the mechanism for high critical temperature remains essentially unknown, in part due to the difficulties in describing accurately their electronic structure; however, there are strong indications that it is related to the magnetic structure.[16,17] The recent discovery of superconductivity in a new family of compounds derived from LaOFeAs[18,19] has renewed interest in strongly correlated magnetic solids and stimulated further research. In the case of cuprates, the strong correlation in the $3d$ shell provokes the unpaired electrons to be essentially localized at the Cu^{2+} site leading to an antiferromagnetic insulator. Recently, it has been suggested that the electronic structure of the LaOFeAs parent compounds has strong similarity with that of the cuprates, being described as a strongly frustrated antiferromagnetic insulator.[20] However, this similarity only emerges when the description of the electronic structure of this material arises from methods that go well beyond LDA and GGA approximations to the unknown universal exchange-correlation functional of DFT. In fact, the lack of wave-function methods (other than Hartree-Fock[21,22] and second-order perturbation theory[23,24] based methods) fully exploiting translational symmetry or making use of appropriate periodic boundary conditions, makes DFT the standard approach to explore the electronic structure of solids, with most applications relying precisely on LDA and GGA methods. However, we already mentioned that LDA and GGA fail to describe the antiferromagnetic insulating character of the electronic structure of strongly correlated systems and, in particular, of high-T_c superconducting parent compounds and predict them to be metallic conductors. In some cases, this deficiency of LDA and GGA can be remedied by directly introducing a correction to the LDA or GGA potential. This is the case of the LDA+U or GGA+U methods,[25] which are able to correctly describe the antiferromagnetic insulating ground state of strongly correlated systems such as Ce_2O_3 (Ref. 26) or LaOFeAs (Refs. 20 and 27), but at the cost of incorporating parameters that are external to the theory and material-dependent. In addition, recent work has shown that these approaches still have difficulties in describing the mag-

netic coupling in molecules.[28] Other approaches attempting to overcome the LDA deficiencies by correcting for self-interaction error such as LDA+SIC (Ref. 29) or GW approximations.[30] In particular, it has been shown that the GW approximation works extremely well for many different strongly correlated materials.[31–33]

Hybrid functionals,[34–36] mixing a part of exact nonlocal Fock exchange with the exchange part of the LDA or GGA potential, provide a good alternative to LDA and GGA. In particular, the broadly used Becke-three-parameter-Lee-Yang-Parr (B3LYP) hybrid functional[34,37] was initially introduced to reproduce the thermochemistry of spectroscopic properties of a large set of organic molecules[38,39] but has been shown to properly describe transition metal containing molecules,[40] dinuclear complexes,[41] and magnetic solids.[42,43] More importantly, B3LYP and related hybrid functionals provide a qualitatively correct description of many different structural, electronic, and magnetic properties of a paradigmatic magnetic insulator such as NiO (Ref. 13) with predicted band gaps which are close to experiment.[44–46] Hybrid exchange-correlation potentials including a contribution of Fock exchange of 20–35 %, such as B3LYP or PBE0,[34–36] properly describe the magnetic coupling in strongly correlated systems such as NiO,[13] $NKiF_3$, and K_2NiF_4,[42,43,47] and La_2CuO_4,[42,43] $LaMnO_3$,[48] and MnO (Ref. 49) among others, which are all prototype materials where standard LDA and GGA fail.[50–52] Unfortunately, the B3LYP functional consistently overestimate the magnetic coupling constant in molecules and solids,[53,54] a problem which emerges clearly when spin symmetry is imposed to the density-functional calculations of molecular systems or of magnetic solids represented by appropriate embedded-cluster models.[55–58]

Recent developments on exchange-correlation potentials have shown that it is possible to reach a more accurate description without having to impose explicitly spin symmetry conditions.[59,60] A detailed analysis of the short- and long-range decay of the hybrid potentials by Scuseria and collaborators[61] has shown that in metallic systems the nonlocal exchange interaction has an extremely slow spatial decay, which has undesired numerical and physical effects in systems with small or vanishing band gaps. In addition, the asymptotic decay of the exchange potential for atomic and molecular systems is incorrectly described by the commonly used hybrid functionals such as B3LYP.[62,63] In order to solve these problems, Vydrov *et al.*[64] implemented and tested[64,65] a long-range corrected hybrid method based on the PBE GGA functional, hereafter denoted as LC-ωPBE, which follow earlier ideas aimed at restoring the proper asymptotic limit.[66,67] For a large number of applications, including molecular structure, thermochemistry, energy barriers and long-range charge-transfer processes, the LC-ωPBE functional shows overall improvement over standard hybrids such as PBE0[35,36] or B3LYP. Likewise, Heyd, Scuseria, and Ernzerhof have presented a short-range corrected hybrid functional (HSE) which properly describes metallic systems.[68] The HSE functional is particularly accurate in estimating band gaps of solids.[69–72] HSE properly describes ceria and reduced ceria.[73]

The excellent performance of range-separated hybrid functionals in describing a variety of chemical systems, and such a delicate property as the magnetic coupling in organic diradicals and transition-metal binuclear complexes,[60] prompted us to analyze their performance in describing different strongly correlated magnetic solids. Hence, the goal of this paper is precisely to explore the performance of the range-separated hybrid functionals for describing the magnetic coupling in prototypal superconducting cuprates parent compounds and transition-metal oxides. For the purpose of the present study, we have found it very convenient to use embedded model clusters for the range-separated hybrids. The correctness of this model has been extensively verified in previous work.[74–76]

This paper is organized as follows: Sec. II describes the appropriate way to define and obtain the magnetic coupling constant from embedded-cluster model calculations using density-functional calculations. The different systems studied and their corresponding models used in the present work are presented in Sec. III. The computational details are outlined in Sec. IV whereas Sec. V reports our results. Finally, Sec. VI summarizes our conclusions.

II. EXTRACTING THE MAGNETIC COUPLING IN MAGNETIC SOLIDS FROM TOTAL-ENERGY DIFFERENCES

A common feature of magnetic systems with n localized unpaired electrons on an atom (or group of atoms) is that these can be regarded as effective spins with total spin quantum number $S=n/2$. In this way, the study of the interactions between effective spins can be analyzed using a spin-only effective Hamiltonian. These model systems allow one to understand the magnetic order leading to spin nets with different topology and dimensionality exhibiting spin dynamics that can be described by the simplest spin effective Hamiltonian which takes the form

$$H^{\mathrm{HDVV}} = -\sum_{i,j} J_{ij}\hat{\mathbf{S}}_i\hat{\mathbf{S}}_j, \tag{1}$$

and it is usually known as the Heisenberg-Dirac-Van Vleck Hamiltonian (HDVV).[77,78] In Eq. (1) $\hat{\mathbf{S}}_i$ and $\hat{\mathbf{S}}_j$ are the effective spin operators in sites i and j, respectively. J_{ij} the magnetic coupling constant and the summation runs over all possible spin pairs although it is often restricted to nearest neighbors or to nearest neighbors and next-nearest neighbors only. For the HDVV Hamiltonian in Eq. (1) one has an antiferromagnetic behavior when the magnetic coupling constant is negative and the low-spin state more stable than high spin. Conversely, a positive value of the magnetic coupling constant favors a ferromagnetic ground state. For systems such as superconducting parent compounds where there is one unpaired electron per Cu site located, the spin operators in the HDVV Hamiltonian correspond to particles with total spin $S=1/2$ whereas for NiO and related systems with two unpaired electrons per Ni site, the corresponding spin operators represent particles with total spin $S=1$. Hence, the HDVV Hamiltonian describes the isotropic interaction between spin moments $\hat{S}_i$ and $\hat{S}_j$ characterizing localized electrons in open shells by means of a set of J_{ij} magnetic coupling constants.

From an experimental point of view, the magnetic coupling constants can be obtained by means of a proper thermodynamic statistics treatment connecting the HDVV solutions with macroscopic properties such as magnetic susceptibility vs temperature measurements, specific-heat capacity vs temperature measurements, or from the intensity of the peaks from magnetic scattering in experiments carried out with spin polarized neutrons. From a theoretical point of view, the J_{ij} magnetic coupling constants can be in general extracted from *ab initio* effective Hamiltonians,[79] although in some cases it is possible to extract them from total-energy differences and make use of the appropriate mapping between the different magnetic states of Eq. (1) and those obtained from suitable first-principles calculations.[54] However, to obtain these energy differences it is necessary to consider a model for the material of interest.

For a crystalline solid, the obvious choice is a periodic model and then the magnetic coupling constant can be extracted from the energy differences between the proper magnetic solutions in the appropriate supercells. In these cases it is convenient to substitute the HDVV Hamiltonian by the Ising Hamiltonian[80] which only takes into account the z component of the spin operators. Hence, one has

$$H^{\mathrm{Ising}} = -\sum_{i,j} J_{ij}\hat{S}_{z_i}\hat{S}_{zj}. \tag{2}$$

Among the different eigenstates of the Ising Hamiltonian one finds the ferromagnetic state (FM) which has the highest possible S_z value, and various antiferromagnetic states (AFM) which have $S_z=0$. A possible criticism to this approach is that the magnetic coupling constant of the HDVV and Ising Hamiltonians could be different. Here, one must realize that most periodic calculations cannot handle spin states because a single Slater determinant does not always allow a well-defined total spin quantum number (per cell or formula unit) which indeed is an observable quantity, and hence these methods provide only the expectation value of the energy for the FM and AFM solutions. While the FM and AFM functions are not spin eigenfunctions, and hence it is not possible to assign a well-defined value to the total spin, they are eigenfunctions of the z component of the total spin operator. Therefore, this observable is well-defined at $T=0$ K and simply corresponds to the total number of alpha electrons minus the total number of beta electrons per unit cell which is fixed in the calculation. Hence, the FM and AFM solutions are eigenfunctions of the Ising Hamiltonian. Moreover, a careful analysis shows that the expectation values of the HDVV and Ising Hamiltonians are the same, thus justifying this approach for obtaining the magnetic coupling constants via total-energy difference of periodic calculations.[54] This becomes clear when the HDVV Hamiltonian is written as in Eq. (3)

$$\hat{H} = -J\sum_{\langle i,j\rangle} \hat{\mathbf{S}}_i \cdot \hat{\mathbf{S}}_j = -J\sum_{\langle i,j\rangle} \left\{ \frac{1}{2}(\hat{S}_{i+}\hat{S}_{j-} + \hat{S}_{i-}\hat{S}_{j+}) + \hat{S}_{zi}\hat{S}_{zj} \right\}, \tag{3}$$

where only one magnetic coupling constant appears because the summation is now restricted to nearest-neighbor magnetic sites. The precise procedure used to derive the equations needed to extract J from periodic calculations depends on the type of magnetic cation and on the topology of the magnetic system resulting from a given crystal structure.[54,74] Let us now consider the spin functions (not spin eigenfunctions) corresponding to the broken-symmetry solutions for a simple-cubic isotropic system with $S=1/2$ to derive the corresponding mapping within the Ising Hamiltonian. For the FM solution, each localized spin moment in a double unit cell has six nearest neighbors, but since each magnetic interaction J involves by definition two magnetic centers, the energy per center is $-6JS_z^2/2$. For the totally AFM solution, the reasoning is the same but the interaction between each pair of spins is now $-J$ and hence the energy is $+6JS_z^2/2$. Therefore one has $E(\mathrm{FM})=-3J/4$, $E(\mathrm{AFM})=+3J/4$, and $E(\mathrm{AFM})-E(\mathrm{FM})=3J/2$. For detailed description on the mapping procedure for periodic systems the reader is referred to the recent work of Rivero *et al.*[81]

In some cases it is not possible to use periodic models either because one wishes to carry out calculations using explicitly correlated wave functions as reported for several systems[16,75,82] or when using state-of-the-art exchange-correlation potentials not yet implemented in periodic codes. For ionic magnetic systems one can design appropriate embedded-cluster models, usually containing two magnetic centers, and extract the magnetic coupling constant also from total-energy differences.[54] In the case of using wave-function-based methods the magnetic coupling constant is directly related to the energy difference between the low-lying-spin states, whereas when using density-functional theory-based calculations, the magnetic coupling constant is related to the energy difference between FM and AFM states as in the periodic case, and the AFM is a broken-symmetry solution. The appropriateness of the embedded-cluster model approach has been established by comparing the values of the calculated magnetic coupling constants of a series of cuprates obtained from periodic and embedded-cluster models.[74–76,83]

III. SYSTEMS AND MODELS

The main goal of the present work is to investigate the performance of range-separated hybrid functionals for describing magnetic coupling constants in a representative set of magnetic materials with different structures, spin, and magnetic orders, and with experimentally known accurate values for the dominant magnetic coupling constants.[84–92] The list of compounds studied in this work includes La_2CuO_4, $KCuF_3$, $KNiF_3$, NiO, and La_2NiO_4. For each of these systems we defined appropriate embedded-cluster models which are described below. There is compelling evidence that these embedded-cluster models provide an extremely good representation of these magnetic systems with magnetic coupling constants computed from accurate configuration-interaction calculations which are in excellent agreement with experiment.[74–76]

The cluster models used in this paper present three different and well-separated regions. The first and second regions are treated quantum mechanically whereas the third region is

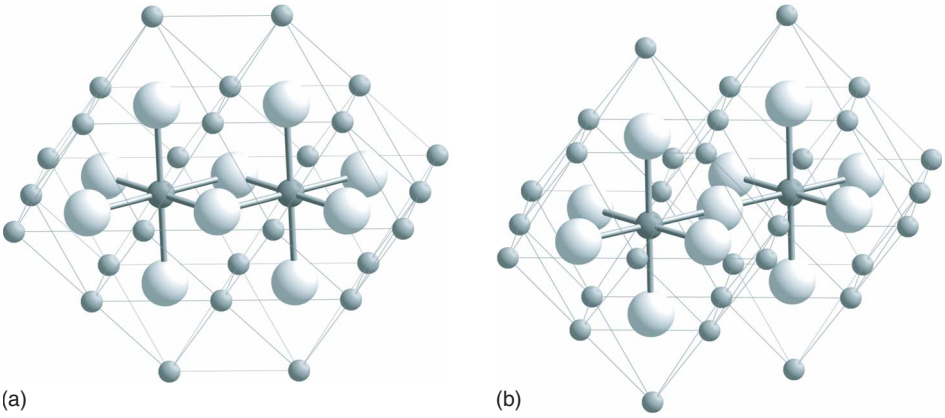

FIG. 1. (Color online) Schematic representation of the Ni_2O_{10} and Ni_2O_{11} moieties defining the first region of the embedded-cluster models, including the TIPs in the second region (small external dark spheres), used to extract the J_1 and J_2 magnetic coupling parameters in NiO.

treated in a classical way. The first quantum region contains two magnetic centers, which here will be either Cu or Ni depending of the system under to study, and the anions (F or O) directly in contact with the magnetic centers. Previous works[16,74–76,82,83] show us that the magnetic coupling constant is a local property involving only the interacting magnetic sites, and the full magnetic interaction is recovered by including their nearest anions. An important remark here concerns the total number of electrons entering in the calculation, which is an external input. The number of electrons is chosen taking into account formal charges for the atoms in the first region although any possible covalent effect is explicitly taken into account when minimizing the energy as a functional of the density. The second quantum region in this model contains a representation of the next-nearest-neighbor cation surrounding the explicit anions in the first region atoms. This representation consist of the cation formal charge plus a potential accounting for exclusion effects between electrons from the first region and the electronic density that one would have in the second region. The resulting entity is usually defined as a Total Ion Potential (TIP). The use of TIPs prevent an artificial polarization of the anion electronic density toward the next-neighbor cations when represented solely by a positive point charge.[93] The TIP consists simply of an appropriate pseudopotential,[94–98] a net charge, and bears no electrons, they constitute a bridge between the first fully quantum mechanical region and the point-charge representation of the rest of the ionic crystal which consists of a sufficiently large array of point charges chosen to provide an accurate representation of the Madelung potential in the central region of the quantum cluster.[99] Note that the final embedded cluster is neutral, not periodic, and conserves crystal point symmetry. The position of the atoms, TIPs, and point charges in the cluster models correspond to the experimental geometry taken from the crystal structures.[84–92] This procedure allows one to investigate the performance of a given computational approach without mixing problems derived from an inaccurate geometry. Note that the magnetic coupling constant is a property extremely sensitive to the distance between the magnetic sites with huge variations resulting from tiny changes in the distances, see for instance Refs. 98 and 100 and references therein.

The embedded clusters used for each system all contain two magnetic centers and their corresponding first-neighbor anions and are built as follows: for La_2CuO_4 the first region is represented by a Cu_2O_{11} cluster model, this is surrounded by 12 TIPs representing the La cations above and below the CuO_2 plane and six TIPS representing the Cu cations connected to the cluster anions in the surface plane and, finally, the Cu_2O_7 plus TIPs are surrounded by an array of 1006 point charges representing the Madelung potential. The first quantum region of the embedded-cluster model for $KCuF_3$ and $KNiF_3$ is Cu_2F_{11} and Ni_2F_{11}, respectively. As described in previous work,[101–103] these quantum clusters are surrounded by 12 TIPs representing K cations and 10 TIPs representing either Cu or Ni, respectively, and the resulting region is surrounded by an array of 430 point charges. Note that for $KCuF_3$, one may have magnetic coupling in the a,b plane or on the c directions. The model just described is used to investigate the coupling through the a,b plane. An identical quantum region is used to investigate the coupling along the c direction but with an array of 560 point charges. For La_2NiO_4 we use a Ni_2O_{11}, 12 La TIPs, 6 Ni TIPs, and 2036 point charges. Finally, let us consider NiO which provides a beautiful example of a system with two different dominant magnetic coupling parameters, a next-nearest-neighbor dominant interaction J_2 along the Ni-O-Ni path involving angles with 180° and a smaller nearest-neighbor interaction J_1 involving a Ni-O-Ni interaction through 90°. In this case one also needs two different clusters which are schematically shown in Fig. 1. These are an embedded Ni_2O_{10} cluster model with 26 TIPS and also 1288 point charges used to extract the J_1 magnetic coupling parameter (Fig. 1(a)) and an embedded Ni_2O_{11} cluster with 30 Ni TIPs and 1288 point charges used to extract J_2. In all cases the magnitude of the charges is chosen according to the formal oxidations state except for charges at the array edge which are chosen according to the Evjen method.[99]

IV. COMPUTATIONAL DETAILS

Density-functional calculations have been carried out for the embedded-cluster models described in the previous section using the well-known and widely used B3LYP functional[34,37] and two-range-separated hybrid functionals. These are the Heyd, Scuseria, and Ernzerhof short-range screened hybrid functional (HSE)[68] and the long-range corrected hybrid functional (LC-ωPBE) of Vydrov and Scuseria.[64] The HSE functional defined as in Eq. (4)

$$E_{xc}^{\mathrm{HSE}}(\omega) = aE_x^{\mathrm{SR\text{-}HF}}(\omega) + (1-a)E_x^{\mathrm{SR\text{-}PBE}}(\omega) + E_x^{\mathrm{LR\text{-}PBE}}(\omega) + E_c^{\mathrm{PBE}}, \quad (4)$$

corrects the PBE GGA functional[104] with a short-range hybrid and allows one to properly describe metallic systems. Values of ω ranging between 0.05 and 0.35 a_0^{-1} have been recommended to obtain good accuracy and computational efficiency when applied to molecules and solids. The optimum value in HSE is ω=0.11 a_0^{-1}.[105] We note that setting ω=0 leads to the hybrid PBE0 functional while for $\omega \to \infty$ the resulting functional is the PBE form of the GGA potential. In HSE, the hybrid aspect of the functional is switched on in the short range only, whereas the PBE GGA functional is used at long electron-electron distances. The physical motivation of HSE is to cut-off the long-range portion of the Hartree-Fock exchange potential which becomes unphysical as the band gap closes. Note, however, that ω=0.11 a_0^{-1} roughly corresponds to a spatial range of 9 Bohrs, which is fairly "long" by most standards and easily includes first and second neighbors. On the other hand, the LC-ωPBE hybrid functional[64] defined as

$$E_{xc}^{\mathrm{LC\text{-}}w\mathrm{PBE}}(\omega) = E_x^{\mathrm{LR\text{-}HF}}(\omega) + E_x^{\mathrm{SR\text{-}PBE}}(\omega) + E_c^{\mathrm{PBE}} \quad (5)$$

has a different physical motivation with molecules in mind (as opposed to solids) and aims to restore the proper asymptotic limit of the molecular exchange-correlation potential. In this approximation, the Fock exchange describes the long electron-electron distances whereas at short range the interaction is that given by the PBE (or similar GGA) functional. The optimum ω=0.40 a_0^{-1} value in LC-ωPBE provides excellent performance for a large number of properties, including molecular structure, thermochemistry, energy barriers, long-range charge-transfer processes,[64,65] and magnetic coupling in molecular systems.[60] Here, setting ω =0 leads to the PBE functional while for $\omega \to \infty$ one gets Hartree-Fock exchange plus the PBE correlation functional. In general, the LC-ωPBE functional has been shown to lead to an overall improvement for molecular properties over standard hybrids such as B3LYP or even HSE. For a more detailed discussion about the importance of Hartree-Fock exchange at different ranges, see Henderson *et al.*[61]

It is interesting to highlight that the HSE and LC-ωPBE functionals rely on opposed definitions of the range at which the Fock exchange is active. At first sight this may seem quite surprising, especially in view of the large improvements over B3LYP results obtained by both range-separated hybrid functionals. However, it appears that HSE and LC-ωPBE work well because the true important region where one needs Fock exchange to describe magnetic effects is the middle-range (MR) region.[61] One can get the MR from the short-range corrected HSE or one can get it from the long-range corrected (LC-ωPBE), but it is the 2–8 a_0 region where some Fock exchange seems important to describe magnetic phenomena correctly. This is in line with recent findings using MR potentials.[61,106] Note also that previous work on molecular magnetic systems shows that, although both HSE and LC-ωPBE functionals largely improve the description achieved by standard hybrids, LC-ωPBE performs noticeably better than HSE. Here, we explore the performance of these two range-separated hybrids in describing magnetic coupling in strongly correlated solids. We recall that the magnitude and sign of J results from a delicate equilibrium between exchange and correlation effects as defined in wave-function-based electronic structure theory. However, the meaning of exchange and correlation in DFT is almost always different since the exchange potential also includes interactions which are typical of electron-electron static correlation effects and would have to be included in the correlation potential. This is clear from the work of Martin and Illas[42,43] precisely on magnetic coupling and from the discussion in our previous work on molecular magnetic systems[60]

DF calculations using the exchange-correlation potentials have been carried out for the embedded-cluster models described in the previous section using standard Gaussian basis sets. For Cu, Ni, O, and F, all electrons are explicitly considered and described by means of large basis sets which are essentially those used in previous work;[42,43] this also applies to the choice of the TIPs in the second region of the embedded cluster. The cluster model calculations have been carried out using a development version of the GAUSSIAN suite of programs.[107]

V. RESULTS AND DISCUSSION

Table I summarizes the results obtained by means of the range-separated hybrid functionals and the embedded-cluster model representation of the materials of interest. Here we compare the results from the present hybrid DFT methods with experimental J values and the precise wave-function based results obtained using the difference dedicated configuration interaction (DDCI3) method.[75] From these results it is clear that both range-separated functionals systematically improve the accuracy with respect to the standard B3LYP hybrid. The improvement affects both ferro- and antiferromagnetic coupling and it is similar for both HSE and LC-ωPBE functionals even if the corrections included in the functional affect different physical contributions. In some materials the predicted results are very close to experiment; this is the case for La_2NiO_4 where the calculated result is only 4% of error with respect to the experimental value. In general, the range-separated functionals predict smaller magnetic coupling constants than B3LYP but still larger than the experimental value. Nevertheless, it is clear that the long-range corrected LC-ωPBE performs considerably better than B3LYP and also than HSE, at least for magnetic coupling, although we must add that LC-ωPBE still tends to overestimate the band gaps whereas HSE leads to values closer to experiment. The performance of these range-separated functionals in describing magnetic coupling in the magnetic solids examined here is in agreement with recent results concerning magnetic coupling in molecular systems.[60] The reduction in the calculated magnetic coupling constant predicted by the range-separated functionals does not mean a

TABLE I. Calculated magnetic coupling constants (J in meV) for the different systems considered in the present work as obtained from the range-separated hybrid HSE and LC-ωPBE functionals applied to the embedded-cluster models. B3LYP and experimental values are included for comparison. Results from accurate configuration-interaction (DDCI3) cluster model calculations from Refs. 82 and 103 and experimental values are included for comparison. Positive and negative values correspond to ferro- and antiferromagnetic couplings, respectively.

		B3LYP	HSE	LC-ωPBE	DDCI3	Experiment
La_2CuO_4		−236.56	−201.75	−185.49	−150.0	−146.0 [a]
La_2NiO_4		−37.93	−32.16	−30.83	−26.9	−31.0 [b]
$KNiF_3$		−15.09	−12.55	−12.94	−7.6	−7.4 [c]
NiO	J_1	+3.39	+2.85	+2.43	1.33	+1.4
	J_2	−30.87	−25.87	−25.29	−16.4	−19.0 [d]
$KCuF_3$	J_{ab}	+3.99	+3.18	+1.85	−0.56	+0.35
	J_c	−57.91	−47.78	−48.94	−28.8	−33.5 [e]

[a]Reference 85.
[b]Reference 86.
[c]Reference 87.
[d]References 88 and 89.
[e]References 90–92.

reduction in the calculated magnetic moment, estimated from the Mulliken analysis of the spin density. In fact, the HSE- and LC-ωPBE-calculated magnetic moments are slightly larger than those arising from the B3LYP potential (Table II). The calculated magnetic moment cannot be directly compared to experiment because it is obtained from the approximate Mulliken population analysis and corresponds to its spin-only component (i.e., neglecting orbital angular-momentum contributions). However, since for a given material the B3LYP, HSE, and LC-ωPBE calculations are carried out using the same model and the same GAUSSIAN basis set, the comparison is meaningful.

In order to have a more quantitative analysis of the performance of these range-separated functionals in predicting magnetic coupling in magnetic solids, we plot in Fig. 2 the calculated values in front of the experimental ones. For the three functionals, B3LYP included, we find a linear trend with R^2 values larger than 0.996 as in Eq. (6)

$$J^{\mathrm{B3LYP}} = 1.6268 J^{\mathrm{exp}} + 1.6531,$$

$$J^{\mathrm{HSE}} = 1.3879 J^{\mathrm{exp}} + 1.7540,$$

$$J^{\mathrm{LC\text{-}\omega PBE}} = 1.2694 J^{\mathrm{exp}} + 0.1020. \quad (6)$$

However, even if the regressions are meaningful, there are substantial differences between the three functionals. The slope of the linear plots in Fig. 2 provides a measure of the accuracy of a given functional, the ideal value being 1.000 and will stand for calculations in perfect agreement with experiment. In a similar way, the independent term is a measure of the systematic deviation since for the perfect agreement one will have a 0.000 value. For the B3LYP the slope of 1.6268 and the 1.6531 value for the independent term indicate that the magnetic coupling constants predicted by this functional present the largest deviation from experiment. Nevertheless, the almost linear trend indicates that relative

TABLE II. Calculated magnetic moments in the antiferromagnetic (AFM) and ferromagnetic states (FM) for the metal atoms (μ in a.u.) in the different systems considered in the present work as obtained from the range-separated hybrid HSE and LC-ωPBE functionals applied to the embedded-cluster models and estimated from the Mulliken population analysis of the spin density. B3LYP values are included for comparison.

		B3LYP		HSE		LC-ωPBE	
		AFM	FM	AFM	FM	AFM	FM
La_2CuO_4		0.68	0.71	0.71	0.73	0.71	0.73
La_2NiO_4		1.81	1.85	1.84	1.87	1.83	1.86
$KNiF_3$		1.79	1.80	1.81	1.82	1.80	1.82
NiO	J_1	1.72	1.72	1.75	1.75	1.75	1.75
	J_2	1.65	1.68	1.67	1.70	1.68	1.67
$KCuF_3$	J_{ab}	0.81	0.81	0.83	0.84	0.83	0.83
	J_c	0.81	0.82	0.83	0.84	0.83	0.83

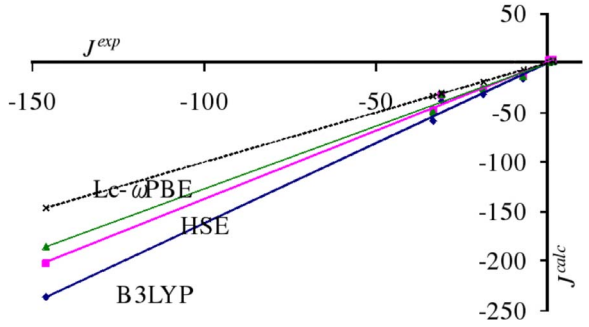

FIG. 2. (Color online) Plot of calculated vs experimental values of the magnetic coupling constants for the materials of interest in the present work. The dashed line corresponds to a perfect fit and is included as reference.

values are well-predicted by this method. For the short-range corrected HSE functional one finds a slope of 1.3879 and an independent term of 1.7540, the former being closer to the ideal value indicating that the corrections included in the functional have a significant effect on the final calculated J values. Finally, for the long-range-separated LC-ωPBE functional one obtains the best description with a slope of 1.2694 and an independent term of 0.1020. However, even in this case the calculated J values are always overestimated by $\sim$25% whereas B3LYP-calculated J values are overestimated by $\sim$60%.

The general improvement of the range-separated functionals and, in particular, of the LC-ωPBE functional, follows the trend recently reported for Cu dinuclear complexes and organic diradicals.[60] However, for these molecular systems the agreement with experiment was slightly better. Reasons for the different behavior in the strongly correlated systems described in the present paper are surely related to the more compact structure which results in a more confined density with the subsequent difficulty to describe the subtle variations through space. In the systems studied here, the distance between the magnetic centers is smaller than in the molecular systems described in Ref. 60 with a much more direct interaction through the bridging ligand. Another possible source of discrepancy may be the choice of the ω parameter. Note that the value used in the present work (ω=0.40) was optimized in molecular studies and it is well possible that solids will require a different treatment. In any case, the fact that improving the functional by improving the physics behind also improves the agreement with experiment provides strong support for the development of new and improved density functionals that may eventually be capable of describing these difficult systems to high accuracy. Note that these are the first set of density-functional results for magnetic coupling which systematically improve the description provided by the B3LYP hybrid functional. In future work, it may be feasible to reoptimize a universal screening parameter ω with magnetic couplings in mind.

An important point concerns the expectation value for the total spin operator $\langle \hat{S}^2 \rangle$ in the ferro- and antiferromagnetic states. For a given material there is no significant difference between the values obtained by means of one or another of the hybrid functionals used in the present work. For the high-spin state it is close to the triplet state for the Cu containing materials ($\langle \hat{S}^2 \rangle \approx 2.0$) and close to the quintet state for the Ni containing compounds, $\langle \hat{S}^2 \rangle \approx 6.0$. For the low spin these values become $\langle \hat{S}^2 \rangle \approx 2.0$ and $\langle \hat{S}^2 \rangle \approx 1.0$ as already commented in the previous section and in line with the arguments from the mapping procedure strongly suggest that the broken-symmetry state used to describe the antiferromagnetic state can be viewed as an almost 50% mixture of high-spin and singlet states.[53,54] Note, however, that pure LDA or GGA functionals may lead to large deviations for these expectation values.[42,43,53,54]

VI. CONCLUSIONS

The performance of the new family of range-separated hybrid density functionals, short-range screened HSE, and long-range corrected LC-ωPBE, for describing the magnetic coupling constant in strongly correlated systems with localized spin moments has been assessed through the study of a broad and representative set of materials including La_2CuO_4 as an example of superconductor cuprate parent compounds, NiO, and La_2NiO_4 as a prototypal transition-metal oxides with rock salt and perovskite structure and, finally, $KCuF_3$ and $KNiF_3$ as examples of transition-metal fluoride perovskites.

The materials studied are represented by suitable embedded-cluster models previously validated.[74–76] The values calculated by means of both HSE and LC-ωPBE represent an overall improvement over the description arising from the standard B3LYP hybrid functionals without large important differences among them but with the LC-ωPBE functional performing noticeably better and leading to results in closer agreement with the experimental J value. Nevertheless, the fact that both HSE and LC-ωPBE perform similarly well strongly suggests that the true important region where Fock exchange is needed to describe magnetic effects is the middle-range (MR).[61] One can get the MR from the short-range corrected HSE or one can get it from the long-range corrected (LC-ωPBE), but it is the 2–8 a_0 region where some Fock exchange seems crucial to describe magnetic phenomena correctly. Moreover, it is worth pointing out that the improvement in the calculated J values by means of these new hybrid functionals arises from a better physical approach to the universal exchange-correlation functional although one must accept that these functionals do also contain some parameters (two in HSE and only one in LC-ωPBE). Nevertheless, the choice of these parameters is driven by physical arguments rather than from agreement to experiment. This is appreciably different from other approaches to hybrid functionals containing several adjustable empirical parameters.

To summarize, range-separated hybrid functionals allow us to reach a more quantitative description of the electronic structure of strongly correlated systems and permits to make accurate predictions of the magnetic coupling constants of

these materials. The improvement over previous functionals relies on physical constraints included in the functional rather than on parameters fitted to experiment. In fact, the increased accuracy of LC-ωPBE suggests that the approximations considered in the definition of this long-range corrected hybrid functional have important consequences for the accurate description of exchange and correlation effects on the electronic structure of magnetic solids and other systems exhibiting localized spins.

ACKNOWLEDGMENTS

P.R. thanks the Spanish *Ministerio de Ciencia e Innovacion* (MICINN) and *Universitat de Barcelona* for supporting his research and stay at Rice University. This work was supported by NSF Grant No. CHE-0807194, by DOE DE-FG02-04ER15523, the Welch Foundation (C-0036), and MICINN Grant No. FIS2008-02238. Calculations were performed on the Rice Terascale Cluster funded by the NSF under Grant No. EIA-0216467, Intel, and HP.

[1] J. G. Bednorz and K. A. Müller, Z. Phys. B: Condens. Matter **64**, 189 (1986).
[2] D. C. Mattis, *The Theory of Magnetism made simple* (World Scientific Publishing Company, Singapore, 2006).
[3] O. Kahn, *Molecular Magnetism* (Wiley-VCH, New York, 1993).
[4] K. Yosida, *Theory of Magnetism, Springer Series in Solid-State Sciences* Vol. 122 (Springer-Verlag, Berlin, 1998).
[5] R. J. Cava, J. Am. Ceram. Soc. **83**, 5 (2000).
[6] E. Dagotto, Rev. Mod. Phys. **66**, 763 (1994).
[7] R. M. Martin, *Electronic Structure, Basic Theory and Practical Methods* (Cambridge University Press, Cambridge, 2004).
[8] P. Hohenberg and W. Kohn, Phys. Rev. **136**, B864 (1964).
[9] S. H. Vosko, L. Wilk, and M. Nusair, Can. J. Phys. **58**, 1200 (1980).
[10] J. P. Perdew and A. Zunger, Phys. Rev. B **23**, 5048 (1981).
[11] J. P. Perdew, J. A. Chevary, S. H. Vosko, K. A. Jackson, M. R. Pederson, D. J. Singh, and C. Fiolhais, Phys. Rev. B **46**, 6671 (1992).
[12] R. G. Parr and W. Yang, *Density Functional Theory of Atoms and Molecules* (Oxford University Press, New York, 1989).
[13] I. de P. R. Moreira, F. Illas, and R. L. Martin, Phys. Rev. B **65**, 155102 (2002).
[14] P. Mori-Sanchez, A. J. Cohen, and W. Yang, Phys. Rev. Lett. **100**, 146401 (2008).
[15] A. J. Cohen, P. Mori-Sanchez, and W. Yang, Science **321**, 792 (2008).
[16] D. Muñoz, F. Illas, and I. de P. R. Moreira, Phys. Rev. Lett. **84**, 1579 (2000).
[17] R. Ofer, G. Bazalitsky, A. Kanigel, A. Keren, A. Auerbach, J. S. Lord, and A. Amato, Phys. Rev B **74**, 220508(R) (2006).
[18] Y. Kamihara, T. Watanabe, M. Hirano, and H. Hosono, J. Am. Chem. Soc. **130**, 3296 (2008).
[19] H. Takahashi, K. Igawa, K. Arii, Y. Kamihara, M. Hirano, and H. Hosono, Nature (London) **453**, 376 (2008).
[20] J. C. Wojdeł, I. de P. R. Moreira, and F. Illas, J. Am. Chem. Soc. **131**, 906 (2009).
[21] R. Dovesi, V. R. Saunders, C. Roetti, R. Orlando, C. M. Zicovich-Wilson, F. Pascale, B. Civalleri, K. Doll, N. M. Harrison, I. J. Bush, Ph. D'Arco, and M. Llunell, *CRYSTAL2006 User's Manual* (University of Torino, Torino, 2006).
[22] K. N. Kudin and G. E. Scuseria, Phys. Rev. B **61**, 16440 (2000).
[23] P. Y. Ayala, K. N. Kudin, and G. E. Scuseria, J. Chem. Phys. **115**, 9698 (2001).
[24] C. Pisani, M. Busso, G. Capecchi, S. Casassa, R. Dovesi, L. Maschio, C. Zicovich-Wilson, and M. Schütz, J. Chem. Phys. **122**, 094113 (2005).
[25] V. I. Anisimov, M. A. Korotin, J. A. Zaanen, and O. K. Andersen, Phys. Rev. Lett. **68**, 345 (1992).
[26] C. Loschen, J. Carrasco, K. M. Neyman, and F. Illas, Phys. Rev. B **75**, 035115 (2007).
[27] G. Giovannetti, S. Kumara, and J. Van den Brink, Physica B **403**, 3653 (2008).
[28] P. Rivero, C. Loschen, I. de P. R. Moreira, and F. Illas, J. Comput. Chem. (to be published).
[29] A. Svane and O. Gunnarsson, Phys. Rev. Lett. **65**, 1148 (1990).
[30] S. Massidda, A. Continenza, M. Posternak, and A. Baldereschi, Phys. Rev. B **55**, 13494 (1997).
[31] M. van Schilfgaarde, T. Kotani, and S. Faleev, Phys. Rev. Lett. **96**, 226402 (2006).
[32] M. Gatti, F. Bruneval, V. Olevano, and L. Reining, Phys. Rev. Lett. **99**, 266402 (2007).
[33] H. Jiang, R. I. Gomez-Abal, P. Rinke, and M. Scheffler, Phys. Rev. Lett. **102**, 126403 (2009).
[34] A. D. Becke, J. Chem. Phys. **98**, 5648 (1993).
[35] C. Adamo and V. Barone, J. Chem. Phys. **110**, 6158 (1999).
[36] M. Ernzerhof and G. E. Scuseria, J. Chem. Phys. **110**, 5029 (1999).
[37] C. Lee, W. Yang, and R. G. Parr, Phys. Rev. B **37**, 785 (1988).
[38] P. J. Stephens, F. J. Devlin, C. F. Chabalowski, and M. J. Frisch, J. Phys. Chem. **98**, 11623 (1994).
[39] L. A. Curtiss, K. Raghavachari, P. C. Redfern, and J. A. Pople, J. Chem. Phys. **106**, 1063 (1997).
[40] F. A. Hamprecht, A. J. Cohen, D. J. Tozer, and N. C. Handy, J. Chem. Phys. **109**, 6264 (1998).
[41] E. Ruiz, P. Alemany, S. Alvarez, and J. Cano, J. Am. Chem. Soc. **119**, 1297 (1997).
[42] R. L. Martin and F. Illas, Phys. Rev. Lett. **79**, 1539 (1997).
[43] F. Illas and R. L. Martin, J. Chem. Phys. **108**, 2519 (1998).
[44] T. Bredow and A. R. Gerson, Phys. Rev. B **61**, 5194 (2000).
[45] J. Muscat, A. Wander, and N. M. Harrison, Chem. Phys. Lett. **342**, 397 (2001).
[46] K. N. Kudin, G. E. Scuseria, and R. L. Martin, Phys. Rev. Lett. **89**, 266402 (2002).
[47] I. Ciofini, F. Illas, and C. Adamo, J. Chem. Phys. **120**, 3811 (2004).
[48] D. Muñoz, N. M. Harrison, and F. Illas, Phys. Rev. B **69**, 085115 (2004).
[49] C. Franchini, V. Bayer, R. Podloucky, J. Paier, and G. Kresse, Phys. Rev. B **72**, 045132 (2005).
[50] K. Terakura, T. Oguchi, A. R. Williams, and J. Kübler, Phys. Rev. B **30**, 4734 (1984).
[51] Z.-X. Shen, R. S. List, D. S. Dessau, B. O. Wells, O. Jepsen, A.

J. Arko, R. Barttlet, C. K. Shih, F. Parmigiani, J. C. Huang, and P. A. P. Lindberg, Phys. Rev. B **44**, 3604 (1991).
[52] H. Sawada, Y. Morikawa, K. Terakura, and N. Hamada, Phys. Rev. B **56**, 12154 (1997).
[53] R. Caballol, O. Castell, F. Illas, J. P. Malrieu, and I. de P. R. Moreira, J. Phys. Chem. A **101**, 7860 (1997).
[54] I. de P. R. Moreira and F. Illas, Phys. Chem. Chem. Phys. **8**, 1645 (2006).
[55] F. Illas, I. de P. R. Moreira, J. M. Bofill, and M. Filatov, Phys. Rev. B **70**, 132414 (2004).
[56] F. Illas, I. de P. R. Moreira, J. M. Bofill, and M. Filatov, Theor. Chem. Acc. **116**, 587 (2006).
[57] I. de P. R. Moreira, R. Costa, M. Filatov, and F. Illas, J. Chem. Theory Comput. **3**, 764 (2007).
[58] C. Adamo, V. Barone, A. Bencini, R. Broer, M. Filatov, N. M. Harrison, F. Illas, J. P. Malrieu, and I. de P. R. Moreira, J. Chem. Phys. **124**, 107101 (2006).
[59] R. Valero, R. Costa, I. de P. R. Moreira, D. G. Truhlar, and F. Illas, J. Chem. Phys. **128**, 114103 (2008).
[60] P. Rivero, I. de P. R. Moreira, F. Illas, and G. E. Scuseria, J. Chem. Phys. **129**, 184110 (2008).
[61] T. M. Henderson, A. Izmaylov, G. E. Scuseria, and A. Savin, J. Chem. Phys. **127**, 221103 (2007).
[62] C. O. Almbladh and U. von Barth, Phys. Rev. B **31**, 3231 (1985).
[63] F. Della Sala and A. Görling, Phys. Rev. Lett. **89**, 033003 (2002).
[64] O. A. Vydrov and G. E. Scuseria, J. Chem. Phys. **125**, 234109 (2006).
[65] O. A. Vydrov, J. Heyd, A. V. Krukau, and G. E. Scuseria, J. Chem. Phys. **125**, 074106 (2006).
[66] Y. Tawada, T. Tsuneda, S. Yanagisawa, T. Yanai, and K. Hirao, J. Chem. Phys. **120**, 8425 (2004).
[67] I. C. Gerber and J. G. Ángyán, Chem. Phys. Lett. **415**, 100 (2005).
[68] J. Heyd, G. E. Scuseria, and M. Ernzernhof, J. Chem. Phys. **118**, 8207 (2003); **124**, 219906(E) (2006).
[69] J. Heyd and G. E. Scuseria, J. Chem. Phys. **120**, 7274 (2004).
[70] J. Heyd and G. E. Scuseria, J. Chem. Phys. **121**, 1187 (2004).
[71] J. Heyd, J. E. Peralta, G. E. Scuseria, and R. L. Martin, J. Chem. Phys. **123**, 174101 (2005).
[72] J. E. Peralta, J. Heyd, G. E. Scuseria, and R. L. Martin, Phys. Rev. B **74**, 073101 (2006).
[73] P. J. Hay, R. L. Martin, J. Uddin, and G. E. Scuseria, J. Chem. Phys. **125**, 034712 (2006).
[74] I. de P. R. Moreira and F. Illas, Phys. Rev. B **55**, 4129 (1997).
[75] I. de P. R. Moreira, F. Illas, C. J. Calzado, J. F. Sanz, J. P. Malrieu, N. B. Amor, and D. Maynau, Phys. Rev. B **59**, R6593 (1999).
[76] F. Illas, I. de P. R. Moreira, C. de Graaf, O. Castell, and J. Casanovas, Phys. Rev. B **56**, 5069 (1997).
[77] W. Heisenberg, Z. Phys. **49**, 619 (1928).
[78] C. Herring, in *Magnetism*, edited by G. T. Rado and H. Suhl (Academic Press, New York, 1965), Vol. 2B.
[79] I. de P. R. Moreira, N. Suaud, N. Guihéry, J. P. Malrieu, R. Caballol, J. M. Bofill, and F. Illas, Phys. Rev. B **66**, 134430 (2002).
[80] E. Ising, Z. Phys. **31**, 253 (1925).
[81] P. Rivero, I. de P. R. Moreira, and F. Illas, J. Phys.: Conf. Ser. **117**, 012025 (2008).
[82] C. de Graaf, C. Sousa, I. de P. R. Moreira, and F. Illas, J. Phys. Chem. A **105**, 11371 (2001).
[83] D. Muñoz, I. de P. R. Moreira, and F. Illas, Phys. Rev. B **71**, 172505 (2005).
[84] G. Aeppli, S. M. Hayden, H. A. Mook, Z. Fisk, S.-W. Cheong, D. Rytz, J. P. Remeika, G. P. Espinosa, and A. S. Cooper, Phys. Rev. Lett. **62**, 2052 (1989).
[85] R. Coldea, S. M. Hayden, G. Aeppli, T. G. Perring, C. D. Frost, T. E. Mason, S.-W. Cheong, and Z. Fisk, Phys. Rev. Lett. **86**, 5377 (2001).
[86] K. Nakajima, K. Yamada, S. Hosoya, T. Omata, and Y. J. Endoh, J. Phys. Soc. Jpn. **62**, 4438 (1993).
[87] M. E. Lines, Phys. Rev. **164**, 736 (1967).
[88] M. T. Hutchings and E. J. Samuelsen, Phys. Rev. B **6**, 3447 (1972).
[89] M. J. Massey, N. H. Chen, J. W. Allen, and R. Merlin, Phys. Rev. B **42**, 8776 (1990).
[90] M. T. Hutchings, E. J. Samuelsen, G. Shirane, and K. Hirakawa, Phys. Rev. **188**, 919 (1969).
[91] S. Kadota, I. Yamada, S. Yoneyama, and K. J. Hirakawa, J. Phys. Soc. Jpn. **23**, 751 (1967).
[92] S. K. Satija, J. D. Axe, G. Shirane, H. Yoshizawa, and K. Hirakawa, Phys. Rev. B **21**, 2001 (1980).
[93] C. Sousa, F. Illas, and G. Pacchioni, J. Chem. Phys. **99**, 6818 (1993).
[94] N. W. Winter and R. M. Pitzer, J. Chem. Phys. **89**, 446 (1988).
[95] R. L. Martin and P. J. Hay, J. Chem. Phys. **98**, 8680 (1993).
[96] R. L. Martin, J. Chem. Phys. **98**, 8691 (1993).
[97] A. B. van Oosten, R. Broer, and W. C. Nieuwpoort, Chem. Phys. Lett. **257**, 207 (1996).
[98] J. Casanovas, J. Rubio, and F. Illas, Phys. Rev. B **53**, 945 (1996).
[99] H. M. Evjen, Phys. Rev. **39**, 675 (1932).
[100] J. Casanovas and F. Illas, J. Chem. Phys. **101**, 7683 (1994).
[101] F. Illas, J. Casanovas, M. A. Garcia-Bach, R. Caballol, and O. Castell, Phys. Rev. Lett. **71**, 3549 (1993).
[102] J. Casanovas and F. Illas, J. Chem. Phys. **100**, 8257 (1994).
[103] I. de P. R. Moreira and F. Illas, Phys. Rev. B **60**, 5179 (1999).
[104] J. P. Perdew, K. Burke, and M. Ernzerhof, Phys. Rev. Lett. **78**, 1396 (1997).
[105] A. V. Krukau, O. A. Vidrov, A. F. Izmaylov, and G. E. Scuseria, J. Chem. Phys. **125**, 224106 (2006).
[106] B. G. Janesko, T. M. Henderson, and G. E. Scuseria, Phys. Chem. Chem. Phys. **11**, 443 (2009).
[107] M. J. Frisch, G. W. Trucks, H. B. Schegel *et al.*, *GAUSSIAN Development Version E.05* (Gaussian, Inc., Wallingford, CT, 2006).